

Specifying the Environments around GRB, Explaining Fe Line in the X-Ray Afterglow of GRB000214

Kei KOTAKE and Shigehiro NAGATAKI

*Department of Physics, University of Tokyo, 7-3-1 Hongo, Bunkyo,
Tokyo 113-0033, Japan*

E-mail: kkotake@utap.phys.s.u-tokyo.ac.jp

E-mail: nagataki@utap.phys.s.u-tokyo.ac.jp

December 2, 2024

Abstract

We present a model explaining the Fe K α line and the continuum in the afterglow of GRB000214. In this paper, we pose the importance to seek the physically natural environment around GRB000214. For the reproduction of the observation, we need the ring-like remnant around the progenitor like that of SN 1987A produced by the mass-loss of the progenitor and the fireball spread over in every directions. The observation of GRB000214, in which the continuum power law spectrum decreased faster than the line, motivated us to consider the two independent systems for the line emission and the continuum spectrum. At first, the continuum spectrum can be fitted by the afterglow emission of the fireball pointing toward the observer which does not collide with the ring because the emission of GRB and the afterglow are highly collimated to the observer by the relativistic beaming effect. Secondly, the line can be fitted by the fluorescence of the Fe atoms in the ring illuminated by the X-ray afterglow. Furthermore, we calculated elaborately the shock interaction between the incoming fireball and the ring to show the thermal bremsstrahlung, which is dominant for the continuum in Boettcher (2000a), is negligible in our model. The significance of this study is that our model may constrain strongly the GRB model. Although the Supranova model in Vietri (1998) assumes the extreme-ring-like remnant produced by the usual supernova explosion, this may not be probable. It is because the supernova remnants are known to be

shell-like. The model also assumes two steps of explosions, on the other hand, we need only one explosion of the progenitor. In this sense, our scenario is more natural. Moreover, in the numerical simulations of Hypernova in Woosley (1993), the jet of the opening angle of only 1 degree is generated. In our model, the fireball which spreads over in every directions reconciles with the observation of 1 % of the polarization in the observation of SN1998bw which showed the explosion might not be so collimated. *KeyWords* : Gamma-rays: Bursts – X-rays: afterglow –supernova remnants – individual (GRB000214)

1 Introduction

There are four Gamma-Ray Bursts (hereafter GRBs) displaying the Fe K α emission lines in their afterglows ([1],[2],[3],[4]). What are the implications of these observations? Fireball model [5], which explains the behaviors of GRBs well, needs a central engine which gives an initial energy input to fireballs. What is a central engine? This has been a long-term mystery and controversial problem. However, with lines in the afterglows, we have an important clue for understanding the environments around GRBs. To construct the model, which explains the line emission, the burst and the afterglow at the same time, are widely interested. So many models, which had been proposed so far before the first line detection in 1997, should be modified to explain the line emission. Amongst them, we categorize them into two. That is to say, binary neutron star merger models [6],[7] and Massive-Star-Related models (e.g., [8],[9],[10]). At first, which sides should we stand? We take the Massive-Star-Related models. It is because binary neutron star merger models, which produce GRBs during the coalescence, take time almost the order of billion years to merge then it happens far away from the star forming regions. It contradicts with the observational facts that GRBs have been often detected in the star forming region

(e.g.,[11],[12]). On the contrary, the following two facts strongly motivate us to consider the Massive-Star-Related models. The first one is that the possible association of GRB 980425 with the type Ic supernova 1998bw was observed [13], in spite of the chance probability for a spatial and temporal coincidence of GRB with the type Ic supernova being less than 10^{-4} . The second one is that the detections of GRBs in the star forming regions have been counted near twenty events as stated above (e.g., [11],[12]).

Now then, which model should we take amongst Massive-Star-Related models? Two well-known scenarios are Supranova model [14],[15] and Hypernova model [8],[9],[10]. In the scenario of Supranova model, at first, the usual supernova explosion creates a rapidly spinning neutron star. Secondly, several months or years later, the neutron star, spinning down by emitting gravitational and electro-magnetic wave, collapses into a Kerr Black hole. Thirdly, the Black holes' rotational energy is converted to power the GRB [16]. They assumed the ring remnants, produced during the supernova explosion. But it may not be probable, since the usual supernovae remnants have shell structures. In addition, if the morphology of the remnant around GRBs is shell-like, fireball will be inevitably scattered by the supernova remnants to decelerate the fireball within one day [17], contradicting year lasting afterglow of GRB970508 and probably shows detectable X-ray absorption lines or emission lines. However, there are no observations like that. In their latest paper [15], they assume a plerionic remnant, but it may be too speculative because of its special morphology. Among Hypernova models ([8],[9],[10]), [8] considered the situation, in which an extended magnetically dominated wind from a GRB impacts the expanding envelope of a massive progenitor to produce the Fe line and the most of

the continuum could still be explained from the standard decelerating fireball. Also in [18], they successfully reproduced the line and the continuum at the same time. Here we suggest an alternative and natural model. We assumed a ring like remnant, which was supported by the HST optical observation of ring-like remnant around SN 1987A [19],[20]. In [11], they discussed a strongly anisotropic GRB environment, that is, a ring. They calculate excellently time evolution of interaction between ring and fireball, and various radiative processes, photoionization, fluorescence, recombination, electron-impact ionization, Compton scattering, bremsstrahlung, Coulomb scattering. As a result, they partially succeeded to reproduce the spectrum of GRB970508. However, the continuum spectrum was dominated by the thermal bremsstrahlung emitted in the shocked region between the incoming fireball and the ring, which was different from the power law continuum obtained in the four above observations with Fe lines. And also, in [21], instead of the fireball, matter of $1M_{\odot}$ and 10^9 cm/s created by Hypernova model [22] is emitted along equatorial plane to hit the ring created during the merger of the progenitors evolved to Helium stars. But also thermal bremsstrahlung was dominant over the spectrum. If the systems of both the line emission region and the continuum flux region are the same, the problem above seems to be still inevitable.

We present the model to reproduce the observation of GRB000214, in which we considered two systems for the line emission and continuum. That is to say, Fe K α line is produced by the fluorescence of the Fe atoms in the equatorial ring illuminated by the X-ray afterglow. On the other hand, the continuum power law flux is obtained by the afterglow emitted from the fireball toward the observer (see, Fig.1). Moreover, we consid-

ered the interaction between the ring and the fireball to investigate whether the thermal bremsstrahlung emission from the shocked region, which was dominant for the continuum in [11], is real or not. As a result, we find the thermal bremsstrahlung emission from the shocked region is negligible by elaborately estimating the temperature behind the shock wave.

In this paper, we propose more clear picture to produce the observational facts, flux level, and spectrum shaping, duration of Fe line. Observational facts of GRB000214 is in section 2. In section 3, physical picture for our model is stated. Discussion are presented in section 4.

2 Observation of GRB000214

We write here the observation of GRB000214 [4]. GRB000214 had a fluence of $F_\gamma = 1.4 \times 10^{-6}$ ergs cm $^{-2}$ and a duration $t_\gamma \simeq 10$ s in the energy band of the Gamma-Ray Burst Monitor on board the *BeppoSAX* satellite (40 - 700 keV). The fluence of the prompt X-ray was 1.0×10^{-6} ergs cm $^{-2}$ (2 keV - 10 keV), which was detected by the Wide Field Cameras also on the *BeppoSAX* satellite. A follow-up observation with the *BeppoSAX* Narrow Field Instruments began about 12 hrs after the corresponding GRB and lasted for 104 ks. The effective exposure time was 51,000 s on source time for *BeppoSAX* Medium-Energy Concentrator/ Spectrometer (MECS) and 15,000 s in the Low-Energy Concentrator/ Spectrometer (LECS), the energy band for each was 1.6 - 10 keV and 0.1 - 4.0 keV. Spectral analysis using the data from MECS and LECS showed that the energy spectrum had a power-law photon index ($\nu^{-\alpha}$, $\alpha = 2.0 \pm 0.3$) and F_x (2 - 10keV)

$= (2.75 \pm 0.9) \times 10^{-13}$ ergs cm $^{-2}$ s $^{-1}$. Line emission was identified with the Fe K α (for hydrogen-like iron) with cosmological redshift of $z = 0.47$. For the Fe line fitting in the spectrum, narrow Gaussian was the best fit, which had a line centroid energy of $E_{\text{line}} = 4.7 \pm 0.2$ keV and $F_{\text{Fe}} = 1.00 - 3.02 \times 10^{-13}$ ergs cm $^{-2}$ s $^{-1}$. The Gaussian fit for emission line was too narrow to find the intrinsic velocity of the matter. For GRB000214 from its narrowness, it can only be inferred that the intrinsic velocity was at most sub-relativistic. We focus on the fact, that the continuum flux decreased more faster than the line flux during the observation of the X-ray afterglow. It motivates us to think the independent systems, for the line emitting region and the continuum emitting region.

3 Physical picture for our model

What is the motivation for our model? As written at the end of section 2, the continuum flux decreased more faster than the line flux during the observation of the X-ray afterglow. And the observed continuum spectrum was power law. If both the line emitting region and the region for the continuum spectrum were supposed to be the same place like in [11], the line disappeared within about one day. In addition, thermal bremsstrahlung emission is dominant. Both of them are not in the cases for the observation of the afterglow of GRB000214. Here we suggest an idea in which the system for the line emitting region and the continuum emitting region are different. That is to say, non-thermal continuum spectrum of GRB000214 [4] can be explained dominantly by the afterglow toward the observer, and the emission of Fe K α line can be explained by fluorescence of the Fe atoms in the ring illuminated by the X-ray afterglow. In our model, we needed the anisotropic

environment around GRB following [11] (see also Fig.1). In addition, we assumed the anisotropic energy deposition of the burst. The anisotropic energy deposition means that the energy per unit solid angle is emitted much stronger along the jet axis toward the observer than other region. Here we should clarify the configuration of the energy deposition. Basically, the fireball is emitted in every directions. To characterize the anisotropic energy distribution of the burst, we introduce two angles, θ in radian and $\delta\Omega$ in steradian, which are explained below. Radiation from relativistically moving matter is beamed in the direction of the motion to within an angle $\theta = \gamma^{-1}$ radian, where γ is the Lorentz factor of the relativistically moving matter. And let $\delta\Omega$ be the angular size (in steradian) of the relativistically moving matter that emits the burst. To keep the total energy minimum, we set $\delta\Omega$ to be equal to $4\pi\gamma^{-2}$. We define E_{jet} , which is the energy emitted within $\delta\Omega \simeq 4\pi\gamma^{-2}$ str in the cone-like region as stated above (see Fig.1). As for the ring, E_{ring} is emitted within $\delta\Theta$ str, which is the covering angle (in steradian) of the ring region. And for the region except the cone-like and ring regions, there is no way to specify the outflow of the energy. It is because it cannot be observed for us owing to the relativistic beaming effect stated above. For the region except the cone-like and ring regions, E_{other} , which is assumed to be

$$E_{\text{other}} = \frac{\delta E_{\text{ring}}}{\delta\Theta} \times (4\pi - \delta\Theta - 2\delta\Omega), \quad (1)$$

is emitted when we calculate the total energy of the system (see section 4). We note both E_{jet} and E_{ring} represent the fireball's kinetic energy. For clarity, we divide physics involved here into two parts to explain the observation of GRB000214. The fireball evolution toward us, which explains well the continuum spectrum, is in 3.1, and the shock

interaction of the fireball with the ring is in 3.2.1, stating the thermal bremsstrahlung emission from the shocked region is negligible. In 3.2.2, the line emission mechanism is stated.

3.1 Parametrization for the continuum afterglow

We analyze the afterglow of GRB000214, following Sari, Piran and Narayan [23]. Seven free parameters required to determine the spectrum in their model are determined below.

$E_{\text{spherical}}$ is given as,

$$E_{\text{spherical}} = \frac{4\pi}{\delta\Omega} E_{\text{jet}} \quad (2)$$

(see Fig.1), which is the kinetic energy of the fireball, estimated as if the explosion were spherical. In fact, if the explosion is jet-like, the intrinsic energy: E_{jet} is much smaller. And, ϵ_B is a parameter, which measures the ratio of the magnetic field energy density to the total thermal energy, ϵ_e is a parameter, which measures the fraction of the total thermal energy which goes into the electrons in the thermal motions, n_{ism} is number density for the interstellar matter, t_d is days from the Burst, γ_0 is initial fireball's Lorentz factor, D is the distance from the GRB center to the observer. Actually from section 2, $t_d = 0.5$, $D = 5.8 \times 10^{27}$ cm, while n_{ism} is set to 1/cc. Then, the numbers of free parameters are reduced to four. We fix $E_{\text{spherical}} = 5.0 \times 10^{52}$ ergs, $\epsilon_B = \epsilon_e = 0.5$, $\gamma_0 = 200$. We notice here that about tenth of $E_{\text{spherical}}$ is emitted as gamma-rays [24]. The radiation of X-Ray afterglow of GRB000214 is specified as adiabatic and fast cooling with the above parameters (e.g.,[23]). We explain it shortly below.

Types	Adiabatic Hydrodynamics	Radiative Hydrodynamics
Slow Cooling	Arbitrary ϵ_e	impossible
Fast Cooling	$\epsilon_e \leq 1$	$\epsilon_e \simeq 1$

Table1 : Classification of the X-Ray afterglow emission (e.g.,[24]) .

The radiation of GRB afterglows is generally divided into three types (see Table 1). At first, we determine whether the radiation is fast or slow cooling. To do this, we are required to prepare the two quantities, γ_c , and γ_m . Both of them are given like below.

$$\gamma_c = \frac{3m_e}{16 \epsilon_B \sigma_T m_p c t \gamma_0^3 n_{\text{ism}}} \quad (3)$$

If a single electron with Lorentz factor : γ_c loses its all kinetic energy by the synchrotron radiation, it means that the electrons with Lorentz factor greater than γ_c are rapidly cooled. On the other hand, as in [24],

$$\gamma_m \simeq 610 \epsilon_e \gamma_0. \quad (4)$$

Above γ_m , the number density of electrons: $N(\gamma)$ accelerated behind the shock obeys power law as $N(\gamma) \propto \gamma^{-p} d\gamma$, ($\gamma \geq \gamma_m$). If $\gamma_c \leq \gamma_m$, it is fast cooling, because the large amount of the electrons are rapidly cooled down by the synchrotron radiation. On the contrary, if $\gamma_m \leq \gamma_c$, it is a slow cooling, only small fraction of the electrons can be cooled. In our case, it is the fast cooling with the above parameters. Next, we determine whether the radiation is radiative or adiabatic. To do this, we need the quantity ϵ_e , which is the fraction of the total thermal energy e which goes into the energy : U_{electron} of the electrons in the random motions, and given as

$$\epsilon_e = \frac{U_{\text{electron}}}{e}. \quad (5)$$

As the exact value of ϵ_e cannot be determined from the observation, it is a free parameter. We set $\epsilon_e = 0.5$ to fit the observation. In the end, we conclude the radiation is adiabatic and fast cooling. For the adiabatic and fast cooling blast wave from [23] ,

$$\nu_c = 1.2 \times 10^{12} \epsilon_B^{-3/2} \left(\frac{E_{\text{spherical}}}{5 \times 10^{52} \text{ergs}} \right)^{-1/2} \left(\frac{n_{\text{ism}}}{1/\text{cc}} \right)^{-1} t_d^{-1/2} \text{ Hz.} \quad (6)$$

$$\nu_m = 1.3 \times 10^{15} \epsilon_B^{1/2} \epsilon_e^2 \left(\frac{E_{\text{spherical}}}{5 \times 10^{52} \text{ergs}} \right)^{1/2} t_d^{-3/2} \text{ Hz.} \quad (7)$$

$$F_{\nu, \text{max}} = 1.7 \times 10^6 \epsilon_B^{1/2} \left(\frac{E_{\text{spherical}}}{5 \times 10^{52} \text{ergs}} \right) \left(\frac{n_{\text{ism}}}{1/\text{cc}} \right)^{1/2} \times \left(\frac{D}{5.8 \times 10^{27} \text{cm}} \right)^{-2} \mu\text{Jy.} \quad (8)$$

where ν_c and ν_m correspond to the relevant Lorenz factor γ_c and γ_m for the observed energy range of 2 - 10 keV. The flux of the afterglow, F_x can be estimated as

$$F_x = \left(\frac{\nu_m}{\nu_c} \right)^{-1/2} \left(\frac{\nu}{\nu_m} \right)^{-p/2} F_{\nu, \text{max}} \text{ ergs cm}^{-2} \text{s}^{-1} \text{Hz.} \quad (9)$$

, where we take the value of p to 4 to fit the observation. In Fig.2, we can fit the observed continuum spectrum well. Near 1 keV, it may seem that the spectrum is different. But it is due to the absorption (Murakami, private communication). So, essentially, the spectrum is a good reproduction of the observation.

3.2 Parametrization of the interaction between the fireball and the ring

We divide this subsection into two to explain the Fe line from the shocked ring. At first, we state the thermal history of the ring, secondly, the line emission mechanism.

3.2.1 Thermal history of the ring

We parameterize the ring. We assume the ring mass, $M_{\text{ring}} = 9.0 \times 10^{32} \text{ g}$, and the inner radius : $R_{\text{in}} = 3.0 \times 10^{15} \text{ cm}$, a tenfold iron overabundance with respect to the solar abundance : $A_{\odot, \text{Fe}} = 10$, the energy shedding towards the ring : $E_{\text{ring}} = 3.4 \times 10^{51} \text{ ergs}$ as the fireball's kinetic energy, the covering angle : $\phi = 50$ degrees (see Fig.1), width of the ring : $\delta R = 3.0 \times 10^{15} \text{ cm}$, which is from the duration of the observation lasting about 100ks. From the observation, R_{in} is determined by the time lag by about one day time lag between the occurrence of GRB and the appearance of Fe line.

$$R_{\text{in}} = c \frac{1 \text{ day}}{T_{\text{time-lag}}} = 3 \times 10^{15} \text{ cm} \quad (10)$$

The fireball emit GRB at $R_{\gamma} \simeq 10^{12} \text{ cm}$ and the afterglow at $R_{\text{afterglow}} \simeq 10^{14} - 10^{15} \text{ cm}$, provided one hundredth of the number density of the ring prevails to $R \simeq 10^{14} \text{ cm}$. (e.g., [23]).

After the half day since the ignition of the fireball, powered by the explosion energy E_{ring} , the fireball with the initially loaded mass of M_0 hits the ring. If we define R_d , where the fireball sweeps the amount of mass ($\simeq \frac{M_0}{\gamma_0}$), then $t_{\text{sub-rela}}$ seconds after the interaction, the blast wave will be decelerated to sub-relativistic speed (e.g., [25]).

$$R_d = \left(\frac{3 E_{\text{ring}}}{4\pi \cos \phi n_{\text{ring}} m_p c^2 \gamma_0^2} + R_{\text{in}}^3 \right)^{1/3} \simeq 10^{15} \text{ cm} \quad (11)$$

and

$$t_{\text{sub-rela}} \simeq \frac{R_d - R_{\text{in}}}{c} = 1.2 \times 10^{-2} \text{ s} \quad (12)$$

It shows before $t_{\text{sub-rela}}$ seconds, the ultra-relativistic behavior of the shocked fluids can be described by Blandford-McKee solution [26], and after $t_{\text{sub-rela}}$, it can be described by

Sedov-Taylor solution. We should estimate the temperature in the two regions, that is to say, that of ultra-relativistic region (hereafter U.R.R), and of Newtonian region (hereafter N.R). At first, for U.R.R, the energy density and the number density of the shocked region are estimated analytically as [24],

$$e(r, t) = 4 n_{\text{ring}} m_p c^2 \gamma(t)^2 \{1 + 16\gamma(t)^2 (1 - r/R)\}^{-17/12}, \quad (13)$$

$$n(r, t) = 4 n_{\text{ring}} \gamma(t) \{1 + 16\gamma(t)^2 (1 - r/R)\}^{-5/4}. \quad (14)$$

where R is the distance of the shock wave measured from R_{in} , r is the distance of the matter behind the shock wave measured from R_{in} , and $\gamma(t)$ is the Lorentz factor of the shock wave in the rest frame of the unshocked ring. Both of them can be estimated from E_{ring} and n_{ring} like below as in [24],

$$\gamma(t) = \frac{1}{4} \left(\frac{17 E_{\text{ring}}}{\pi n_{\text{ring}} m_p c^5 t^3 \cos \phi} \right)^{1/8} \quad (15)$$

$$R(t) = \left(\frac{17 E_{\text{ring}} t}{\pi m_p n_{\text{ring}} c \cos \phi} \right)^{1/4} \quad (16)$$

On the other hand, the energy density of the nucleus in the shocked region at the given temperature is given below.

$$e(r, t) = \frac{3}{2} n(r, t) k_B T_{\text{shocked ring}} \quad (17)$$

Equating the equation (13) with (17), we can estimate the upper limit of the temperature in the shocked region by setting $r = R$. For the U.U.R,

$$\begin{aligned} T_{\text{U.R.R}} &= 2.0 \times 10^{12} \left(\frac{E_{\text{ring}}}{3.4 \times 10^{51} \text{ergs}} \right)^{1/8} \left(\frac{n_{\text{ring}}}{1.4 \times 10^9 / \text{cc}} \right)^{-1/8} \\ &\times \left(\frac{t}{8 \times 10^4 \text{s}} \right)^{-3/8} \left(\frac{\sec \phi}{\sec 50^\circ} \right)^{1/8} \text{ K.} \end{aligned} \quad (18)$$

Also for the N.R,

$$T_{\text{N.R.}} = 1.0 \times 10^{12} \left(\frac{E_{\text{ring}}}{3.4 \times 10^{51} \text{ergs}} \right)^{2/5} \left(\frac{n_{\text{ring}}}{1.4 \times 10^9 / \text{cc}} \right)^{-2/5} \times \\ \left(\frac{\sec \phi}{\sec 50^\circ} \right)^{2/5} \left(\frac{t}{8 \times 10^4 \text{s}} \right)^{-6/5} \text{K.} \quad (19)$$

In [11], the temperature of the shocked region was estimated to be 10^8 K, assuming the total kinetic energy of the incoming fireball was roughly equal to the total thermal energy in the shocked region. However, for the explicit description of the thermal history of the ring, it is inevitable to deal with the shock. Therefore, we solve the shock dynamics analytically to estimate the temperatures of the shocked regions, which are classified into two cites, that is to say, U.R.R and N.R. For the thermal bremsstrahlung emission in the shocked region, the intrinsic emissivity is given as, [27]

$$\varepsilon_{\nu}^{ff} = 5.1 \times 10^{-26} \sum_{k=1}^{26} \left(\left(\frac{\sum_{j=1}^{26} Z_j X_j n_{\text{shocked ring}}}{A_j} \right) \times \right. \\ \left. \frac{Z_k^2 X_k}{A_k} n_{\text{shocked ring},k} \right) T_{\text{N.R.}}^{-1/2} \times \\ \exp \left(\frac{-h \nu}{k_B T_{\text{N.R.}}} \right) \text{ergs cm}^{-3} \text{s}^{-1} \text{Hz}^{-1}, \quad (20)$$

, where the summation are taken from $j=1$ (hydrogen) to $j=26$ (iron), and $Z_j, X_j, n_{\text{shocked ring},j}$ represent electron number, mass fraction, the number density of the j species of nucleus, and the gaunt factor is excluded in the equation (20), which is an order of unity (e.g., [27], page 161). We remark that both $n_{\text{shocked ring}}$, and $T_{\text{shocked ring}}$ in equation (20) are the quantities estimated in the N.R region, because after $t_{\text{sub-rela}}$, the dynamics of the shock wave can be described by the Sedov-Taylor solution. For the temperature in the equations (18) and (19), the thermal bremsstrahlung emission from the shocked region is negligible

(see Fig2). It is because under the relevant temperature, the energetic electrons cannot be bent by the Coulomb interaction with the nucleus, leading the emissivity of the thermal bremsstrahlung lower. And the fluorescent line emission will be suppressed, since all the nucleon will be ionized under the temperature for the production the fluorescent line. Therefore if the line emitting region and the continuum emitting region are the same like in [11], neither the continuum nor the line can be explained. In our model, the problem can be resolved to take the two systems for the line emitting region and the continuum emitting region into consideration. In our model, the continuum can be determined only by the afterglow pointing toward us (see Fig.2).

3.2.2 Line emission mechanism

For Fe $K\alpha$ emission, three mechanisms are proposed by [17], namely, fluorescence in optically thin ring, thermal emission from the ring and reflection (see Fig.1 in [17]). In our model, Fe $K\alpha$ line is produced by the fluorescence scenario, because the others have the problems. In the model of thermal emission from the ring, if the ring is thermalized by the shocked region to produce the line emission, it contradicts with the observation as stated in the beginning of section 3. In the model of reflection, the line is explained by the fluorescent Fe line near the surface of the ring, if the ring is optically thick to the photons of the X-ray afterglow. However, just after the arrival time of the burst photon, the fireball will hit the ring leading the non-thermal plasma for the fluorescent line to the thermal plasma. Thus it seems difficult to explain the line by the reflection model. For GRB000214, to avoid the problem, we considered a slightly ionized Fe atoms in the optically thin plasma. We emphasize here that the fluorescence comes from the optically

thin region. As stated in subsection 3.2.1, after $t_{\text{sub-rela}} \simeq 1 \times 10^{-2}$ seconds the shock wave becomes non-relativistic and the dynamics of the shock can be described by the Sedov Taylor solution. Therefore, the radii of the shocked wave, which can reach after one day from the burst, can be estimated as,

$$R_{\text{shock}} = R_{\text{in}} + R_{\text{N.R. one day}} = 4.7 \times 10^{15} \text{ cm} \quad (21)$$

Thus, the effective volume : $V_{\text{emitting region}} = 1.9 \times 10^{47} \text{ cm}^3$ for the fluorescence is about half of the total volume of the ring, on the other hand, the volume of shocked region is $V_{\text{shocked region}} = 2.1 \times 10^{47} \text{ cm}^3$. The shock wave has passed half of the total volume of the ring, in which the plasma in the ring are thermalized not to emit the line by the fluorescence. The time evolution of the fluorescence is stated roughly in the following. At first, photons from the X-ray afterglow are absorbed in the ring to render the electrons in the neutral Fe atoms ionized. Secondly, fluorescent K α line is emitted by the transition of the electrons. The process of making the fluorescence line is effective at the time when the ring is illuminated not by the prompt burst, but by the X-ray afterglow. It is because the recombination time-scale for explaining the observed line should be less than 1×10^{-7} seconds if the line is produced by the prompt gamma-rays, on the other hand, the recombination time-scale during the prompt gamma-rays is less than hundred seconds (e.g.,[17]). So we find that line cannot be produced by the prompt gamma-rays. As we state in the following in detail, the recombination time required for the line is not so short for the X-ray afterglow. To explain the line flux by fluorescence, we demand the two conditions. The first one is that the plasma in the ring should not be fully ionized, it is because if the region is fully ionized, line should not be emitted. The second one is that

the optical depth for the line should be an order of unity. It is because if the region is optically thick to the line photons, we cannot observe the line. In the following, we refer to the above two conditions. The first one is that the plasma in the ring illuminated by the X-ray afterglow, should not fully ionize the plasma. For determining the ionization state of plasma, which is illuminated by the incoming photons, we have only to compare the ionization time scale t_{ion} with t_{rec} . For the purpose, we should specify the temperature of the ring after the illumination by the X-ray afterglow. The heating rate: Γ can be estimated as [28],

$$\begin{aligned}\Gamma &= \frac{n_{\text{Fe, K}}}{4\pi R_{\text{in}}^2 \cos \phi} \int_{\epsilon_{\text{Fe, K}}}^{\infty} \sigma_{\text{Fe, K}}(\epsilon - \epsilon_{\text{Fe, K}}) \frac{dL}{d\epsilon} \frac{d\epsilon}{\epsilon} \\ &= 2.4 \times 10^{-2} \left(\frac{R_{\text{in}}}{3 \times 10^{15} \text{cm}} \right)^{-2} \left(\frac{n_{\text{ring}}}{1.4 \times 10^9 / \text{cc}} \right) \left(\frac{E_{\text{ring}}}{3.4 \times 10^{51} \text{ergs}} \right) \left(\frac{A_{\odot, \text{Fe}}}{10} \right) \left(\frac{\sec \phi}{\sec 50^\circ} \right) \\ &\quad \text{erg cm}^{-3} \text{ s}^{-1}.\end{aligned}\quad (22)$$

, where $\sigma_{\text{Fe, K}}$ is the approximated photoionization cross section [29],

$$\sigma_{\text{Fe, K}} = 9.3 \times 10^{-21} \left(\frac{\epsilon}{\epsilon_{\text{K}}} \right)^{-3} \text{cm}^2 \quad (23)$$

, $\epsilon_{\text{Fe, K}}$ is the edge energy of Fe K : 7.5 keV, and L is the luminosity of the X-ray afterglow. The quantity of t_{ill} , which is the illumination time by the X-ray afterglow of the ring, can be estimated as,

$$t_{\text{ill}} = \frac{R_{\text{in}}}{2 \gamma_0^2 c} \text{ s.} \quad (24)$$

The temperature of the illuminated ring : $T_{\text{illuminated ring}}$ can be estimated as ,

$$\Gamma t_{\text{ill}} = \frac{3}{2} n_{\text{ring}} k_{\text{B}} T_{\text{illuminatedring}} \text{ erg}^3 \text{ cm}^{-3}. \quad (25)$$

and,

$$T_{\text{illuminated ring}} = 3.3 \times 10^5 \left(\frac{R_{\text{in}}}{3 \times 10^{15} \text{cm}} \right)^{-2} \left(\frac{E_{\text{ring}}}{3.4 \times 10^{51} \text{ergs}} \right) \left(\frac{\sec \phi}{\sec 50^\circ} \right) \left(\frac{A_{\odot, \text{Fe}}}{10} \right) \text{K.} \quad (26)$$

We can estimate recombination time-scale for the Fe ka line as [31],

$$t_{\text{rec}} = 1.0 \times 10^{-3} \left(\frac{n_{\text{ring}}}{1.4 \times 10^9 / \text{cc}} \right)^{-1} \frac{1}{\alpha(\lambda)} \text{ s.} \quad (27)$$

, where

$$\alpha(\lambda) = 1.4 \times 10^{-12} \lambda^{1/2} (0.5 \ln \lambda + 4.2 \times 10^{-1} + \frac{5.0 \times 10^{-1}}{\lambda^{1/3}}) \text{ cm}^{-3} \text{ s}^{-1}, \quad (28)$$

and where λ is given as,

$$\lambda = 3.2 \times 10^2 \left(\frac{R_{\text{in}}}{3 \times 10^{15} \text{cm}} \right)^2 \left(\frac{\sec \phi}{\sec 50^\circ} \right)^{-2} \left(\frac{A_{\odot, \text{Fe}}}{10} \right)^{-1} \times \left(\frac{E_{\text{ring}}}{3.4 \times 10^{51} \text{ergs}} \right)^{-1}. \quad (29)$$

On the other hand, t_{ion} can be estimated as [28]

$$\begin{aligned} t_{\text{ion}} &= \left(\frac{1}{4 \pi R_{\text{in}}^2 \cos \phi} \int_{\epsilon_{\text{Fe}, \text{K}}}^{\infty} \sigma_{\text{Fe}, \text{K}} \frac{dL}{d\epsilon} \frac{d\epsilon}{\epsilon} \right)^{-1} \\ &= 2.2 \times 10^{-3} \left(\frac{R_{\text{in}}}{3 \times 10^{15} \text{cm}} \right)^2 \left(\frac{E_{\text{ring}}}{3.4 \times 10^{51} \text{ergs}} \right)^{-1} \text{ s.} \end{aligned} \quad (30)$$

, where q is the fraction of the total X-Ray afterglow fluence absorbed by the ring and reprocessed into the line. q can be estimated as (e.g., [32]) as,

$$q = 0.7 \left(\frac{R_{\text{in}}}{3 \times 10^{15} \text{cm}} \right) \left(\frac{n_{\text{ring}}}{1.4 \times 10^9 / \text{cc}} \right) \left(\frac{\epsilon_{\text{edge}}}{\epsilon_{\text{max}}} \right) \left(\frac{0.2}{\epsilon_{\text{edge}}} \right). \quad (31)$$

, where τ_{edge} is the fraction of all photons absorbed between ϵ_{edge} and $2\epsilon_{\text{edge}}$, ϵ_{max} is the maximum energy of the X-ray afterglow, which is an order of several ten keV and

ϵ_{edge} is the edge energy, which is 7.5 keV. With the above two time-scale, we can find that the time-scale for the ionization is comparable with that of recombination. In other words, the plasma is not fully ionized by the incident photons of the X-ray afterglow. We conclude that the fluorescence line is emitted from the non-thermal plasma. Secondly, we demand both the Thomson optical depth, τ_T , and the optical depth of the bound-free transition in the Fe atoms be an order unity for the emitted line photon in the illuminated ring. Because, the large optical depth smears to broaden and vanish the line feature. The optical depth of the Thomson scattering can be estimated as,

$$\tau_T = 6.0 \times 10^{-1} \left(\frac{n_{\text{ring}}}{1.4 \times 10^9 \text{ /cc}} \right) \left(\frac{\delta R_{\text{emitting region}}}{9 \times 10^{14} \text{ cm}} \right). \quad (32)$$

The optical depth for the bound-free transition of a single Fe atom can estimated as (e.g., [33]),

$$\tau_{\text{bf}} = 5 \times 10^{-4} \left(\frac{n_{\text{ring}}}{1.4 \times 10^9 \text{ /cc}} \right) \left(\frac{\delta R_{\text{emitting region}}}{9 \times 10^{14} \text{ cm}} \right) \left(\frac{A_{\odot, \text{Fe}}}{10} \right) \quad (33)$$

Line photons are optically thin to the Thomson scattering and the bound-free transition in the illuminated ring and can escape from the ring without smearing too much the iron line. Hence, we can roughly estimate the line emission by fluorescence. From [17],

$$\begin{aligned} F_{\text{Fe}} = & 1.3 \times 10^{-13} \times \\ & \left(\frac{n_{\text{ring}}}{1.4 \times 10^9 \text{ /cc}} \right)^2 \left(\frac{\frac{\epsilon_{\text{edge}}}{\epsilon_{\text{max}}}}{0.2} \right) \left(\frac{E_{\text{ring}}}{3.4 \times 10^{51} \text{ ergs}} \right) \times \\ & \left(\frac{A_{\odot, \text{Fe}}}{10} \right) \left(\frac{t}{8 \times 10^4 \text{ s}} \right)^{-1} \left(\frac{R_{\text{in}}}{3 \times 10^{15} \text{ cm}} \right)^2 \times \\ & \left(\frac{\frac{V_{\text{emitting region}}}{1.9 \times 10^{47} \text{ cm}^3}}{\frac{V_{\text{emitting region}}}{1.9 \times 10^{47} \text{ cm}^3} + \frac{V_{\text{shocked region}}}{2.1 \times 10^{47} \text{ cm}^3}} \right) \text{ ergs cm}^{-2} \text{ s}^{-1} \end{aligned} \quad (34)$$

As a result, we reproduced the line (see Fig.2).

4 Discussion

We discuss the significance of this study on the mechanism that produces a GRB. No simulations, challenging to explain the stellar collapses and the birth of the GRB at the same time, have succeeded. In the numerical simulations of collapsars (e.g., Woosley 1993), very steep collimation of the jet whose opening angle is about 1 degree is generated. On the contrary, from the observation of SN1998bw, only 1% of the polarization in the optical band was detected, which showed the explosion may not be so collimated. In our model, the fireball should spread over in every directions for illuminating the Fe atoms in the equatorial ring to emit Fe K α line by the fluorescence, which may be consistent with observation. This picture will constrain strongly the GRB models.

We also assumed in this study the existence of the ring which have a tenfold Fe overabundance with respect to the solar abundance. You may have thought that this value is relatively high for the object whose redshift (z) is 0.5. However the GRB are born in the star forming region, the composition of a slightly high metalicity of Fe might be justified.

It is noted that the optical flash of GRB990123 [34] may be explained by the black-body emission from the shocked region of the ring. We will discuss this problem in the forthcoming paper.

Finally, we refer to the amount of the total energy emitted in our system as the kinetic energy of the fireball. We take the initial Lorentz factor as 200, then from the equation (1), $E_{\text{jet}} = 1.25 \times 10^{48}$ ergs within 3.14×10^{-4} str and we can roughly estimate 5.3×10^{51} ergs for the region except the cone region. As a result, the total amount of the kinetic

energy is nearly 10^{52} ergs. This energy is compatible with the usual GRBs.

As a future work, we will perform a series of precise calculations on the ionization states in the ring illuminated by the X-ray afterglow and the ionization states of the plasma in order to investigate the effects of the fluorescence on the line emission in detail. We also regard it as an important task, to pursue the possibility to explain the observation in the case, in which the line emitting region and the continuum emitting region are the same (Masai, Murakami and Yonetoku, private communication).

Acknowledgments

The authors are grateful to Professor K. Masai, Professor H. Murakami and Dr. D. Yonetoku for useful discussions.

References

- [1] Piro L., et al. 1999, *Astrophys. J.*, 514, L73
- [2] Yoshida A. et al. 1999, *A &AS*, 138, 433
- [3] Piro L., et al. 2000, *Science*, 290, 955
- [4] Antonelli L.A. et al. 2000, *Astrophys. J.*, 545, L39
- [5] Rees M.J., Mészáros P. 1992, *MNRAS*, 258, 41P
- [6] Paczyński B., 1986, *Astrophys. J.* 308, L43
- [7] Eishler D., Livio M., Piran T., Shramm D.N. 1989, *Nature*, 340, 126

- [8] Rees M.J., Mészáros P. astro-ph/0010258
- [9] Woosley S.E. 1993, *Astrophys. J.* 405, 177
- [10] Paczyński B., 1988, *Astrophys. J.* 494, L45
- [11] Boettcher M ,2000a, *Astrophys. J* 102, 539
- [12] Dar A astro-ph/0101007
- [13] Galama T.J., et al. 2000, *Nature*, 395, 670
- [14] Vietri M., Perola C., Piro L., Stella L. 1999, *MNRAS*, 308, L29
- [15] Vietri M., Ghisellini G., Lazzati D. 2001, astro-ph/0011580
- [16] Blandford R.D., Znajek R.L. 1977, *MNRAS*, 179, 433
- [17] Lazzati D., Campana S., Ghisellini G. astro-ph/9902058
- [18] Weth C., Mészáros P., Kallman T., and Rees M. 2000, *Astrophys. J.* 534, 581
- [19] Plait C.P., Lundqvist.P., Chevalier R.A., and Kirshner R.P. 1995, *Astrophys. J*, 439, 730
- [20] Lundqvist.P and Fransson.C. 1996, *Astrophys. J.* 464, 924
- [21] Boettcher M., Fryer C.L. ,2000b, *Astrophys. J*, subm. (astro-ph/006076)
- [22] Fryer C.L., Woosley S.E., Hartmann D.H 1999, *Astrophys. J*, 526, 152

- [23] Sari R., Piran T., Narayan R. 1998, *Astrophys. J.*, 497, L17
- [24] Piran T., 1999, *Phys.Rep* 314, 575
- [25] Blandford R.D., McKee C.F. 1976, *Phys.of.Fluids*, 19, 1130
- [26] Kobayashi S., Piran T., Sari R. 1999, *Astrophys. J.*, 513, 669
- [27] Rybicki G. B., Lightman A. P. 1979, *Radiative processes in astrophysics*. John Wiley & Sons, New York.
- [28] Nakayama. M and Masai. K. 2001, in preparation.
- [29] Boettcher M., Dermer C., Cider A., Liang E. 1999, *A&A*, 343, 111B
- [30] Ghisellini G., Haardt F., Campana S., Lazzati D., Covino S., 1999, *Astrophys. J.*, 517, 168
- [31] Verner D.A., Ferland G.J. 1996, *ApJS*, 103, 467
- [32] Ghisellini G., Haardt F., Campana S., Lazzati D., Covino S. 1999, *ApJ*, 168, 517
- [33] Bowers R.L., Deeming T, 1984, *Astrophysics II. Interstellar matter and galaxies*. Boston: Jones and Bartlett
- [34] Sari R., Piran T. 1999, *ApJ*, 517, L109

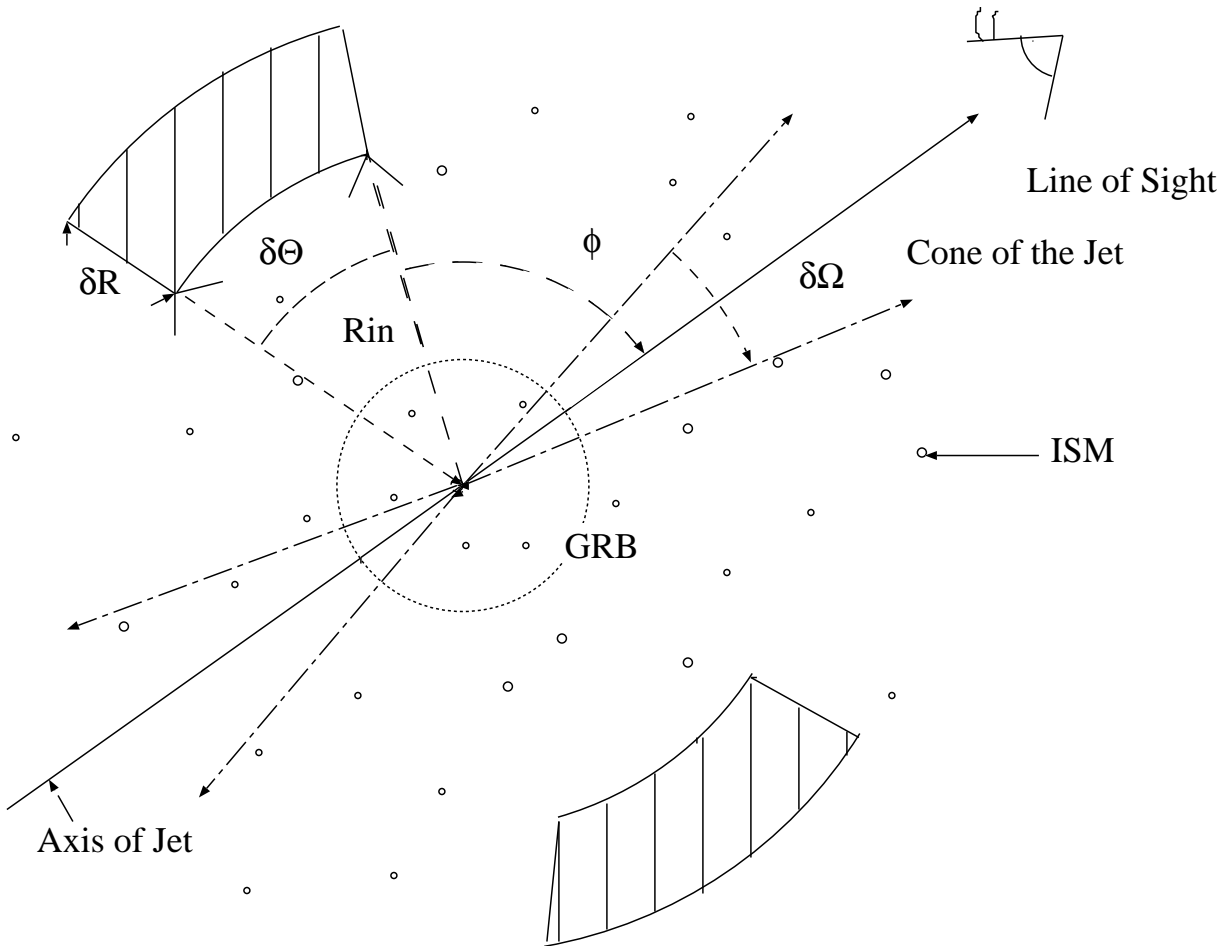


Figure 1: Schematic diagram of the GRB's environment in our model

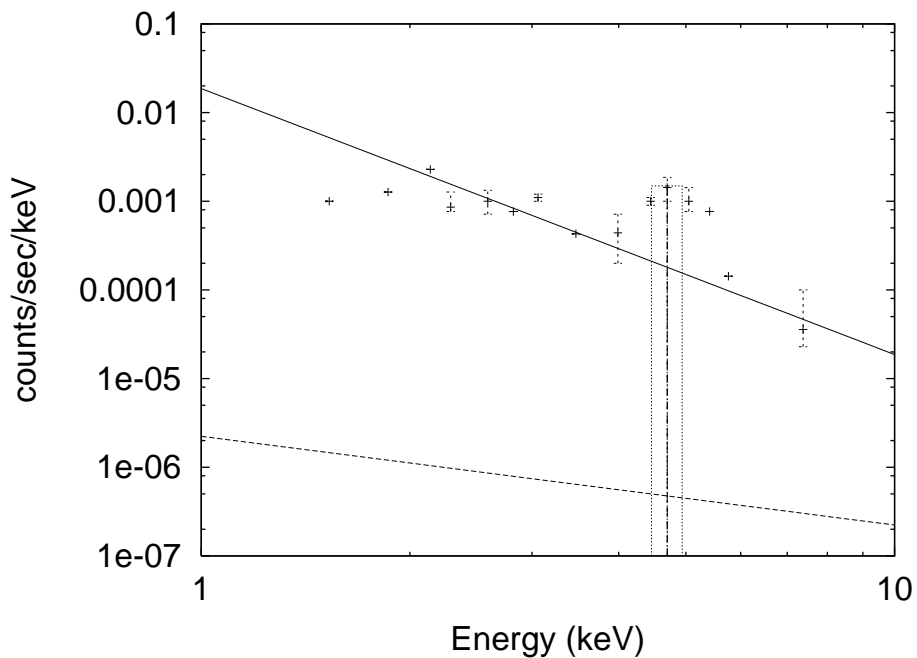


Figure 2: Integrated spectrum, solid line : afterglow emission toward the observer, dashed line : fluorescent line emission of Fe K α originated from the ring illuminated by the X-ray afterglow in the energy bin of 0.48 keV, crosses is the observation of the afterglow and the Fe line in [4]